

## Expanded View Figures

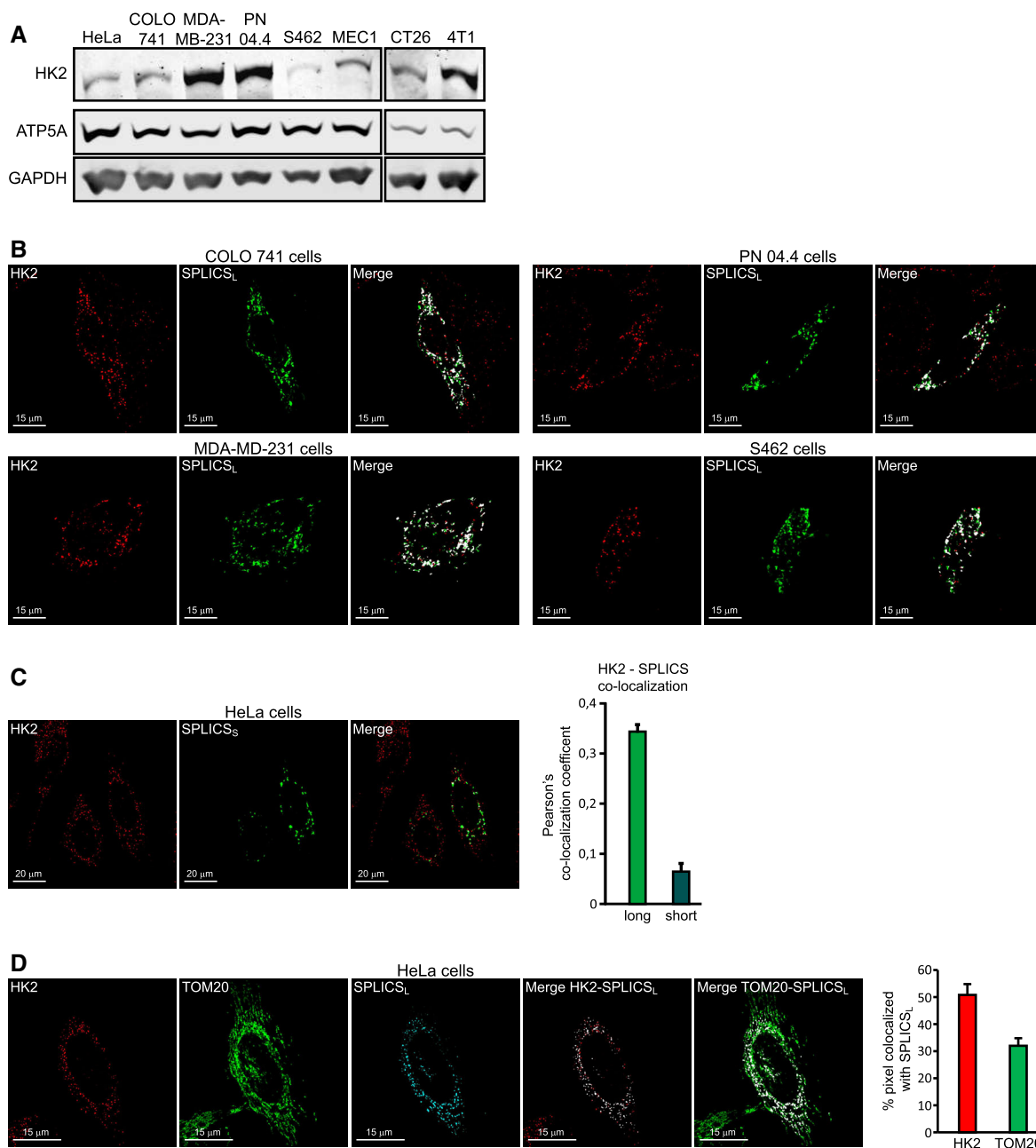
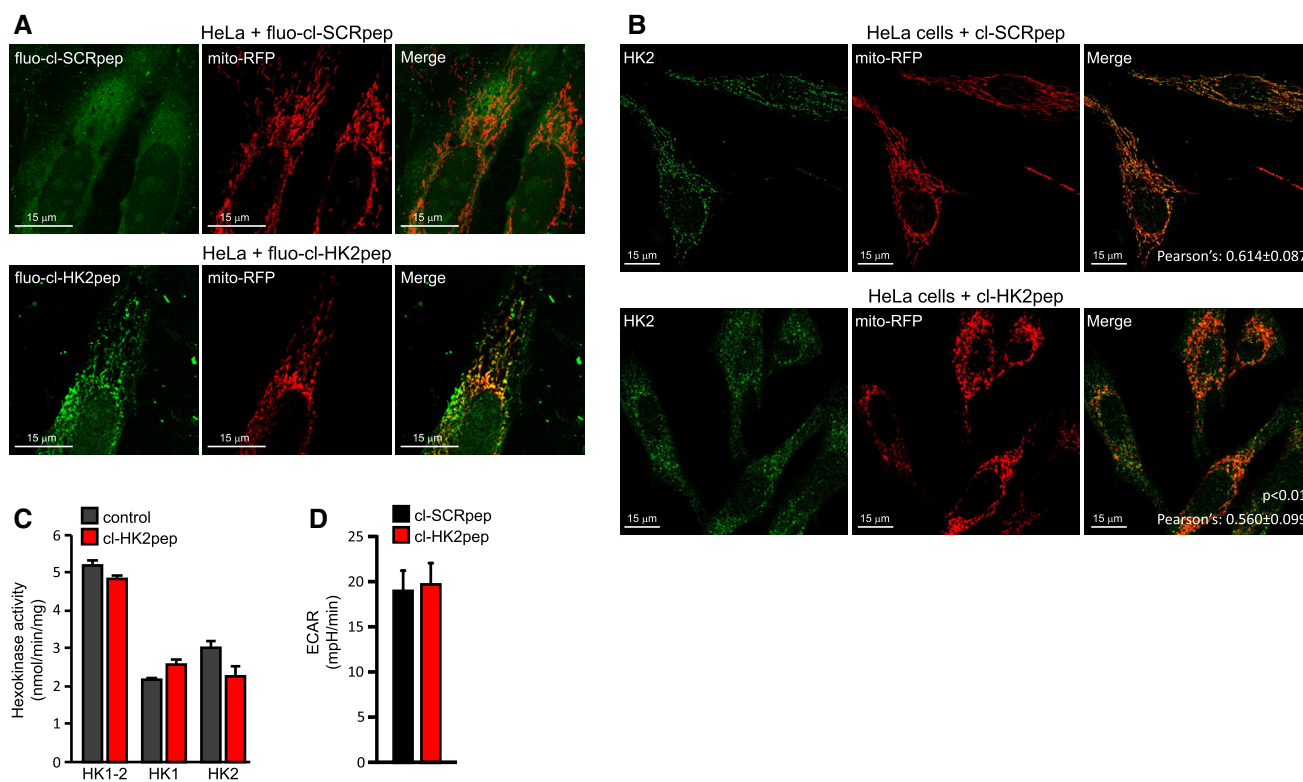


Figure EV1.

**Figure EV1. Related to Fig 1. HK2 locates in MAMs of cancer cells.**

- A Western immunoblot analysis of HK2 expression on neoplastic cells of human origin (cervix carcinoma HeLa cells, colorectal carcinoma COLO 741 cells, breast cancer MDA-MB-231 cells, plexiform neurofibroma PN 04.4 cells, malignant peripheral nerve sheath tumor S462 cells, B-chronic lymphocytic leukemia MEC1 cells) and of mouse origin (colon carcinoma CT26 cells and breast cancer 4T1 cells). ATP5A and GAPDH are mitochondrial and cytosolic loading controls, respectively.
- B Fluorescence co-staining of HK2 and split-GFP-based probe for ER-mitochondria contacts (SPLICS<sub>L</sub>) on colorectal carcinoma COLO 741 cells, breast cancer MDA-MB-231 cells, plexiform neurofibroma PN 04.4 cells, and malignant peripheral nerve sheath tumor S462 cells. HK2 is revealed with an AlexaFluor555-conjugated secondary antibody. Scale bar, 15 μm.
- C Fluorescence co-staining of HK2 and split-GFP-based probe for ER-mitochondria contacts SPLICS<sub>S</sub>. HK2 co-localization with SPLICS<sub>L</sub> (related to Fig 1H) or SPLICS<sub>S</sub> is quantified in the bar graph on the right (mean ± SEM obtained from at least three independent experiments). Scale bar, 20 μm.
- D Both HK2 and the outer mitochondrial membrane marker TOM20 are analyzed for their co-localization with MAMs. HK2 is revealed with an AlexaFluor555-conjugated secondary antibody and TOM20 with an AlexaFluor647-conjugated secondary antibody; the merged signal is white in both analyses. MAM localization of HK2 or TOM20 is quantified in the bar graph on the right (mean ± SEM obtained from three independent experiments). Scale bar, 15 μm.



**Figure EV2. Related to Fig 1. Characterization of cl-HK2pep.**

- A HeLa cells expressing mitochondrial-targeted RFP are treated for 2 min with either cl-SCRpep or cl-HK2pep (1 μM each) labeled with the green fluorophore ATTO 488. The yellow signal indicates mitochondrial localization of the peptide. Scale bar: 15 μm.
- B HK2 displacement from HeLa mitochondria after a 2-min treatment with cl-HK2pep is shown by loss of merging signal analyzed as in Fig 1C. cl-SCRpep is used as a negative control, and Pearson's co-localization coefficient is indicated in figure (cl-SCRpep *n* = 40 cells; cl-HK2pep *n* = 51 cells; *P* < 0.01 with Student's *t*-test). Scale bar: 15 μm.
- C Effect of 10 μM cl-HK2pep on glucose phosphorylation in CT26 cell extracts, where both total hexokinase activity and HK1/HK2-specific activities are measured (mean ± SD, *n* = 3 independent experiments).
- D Extracellular acidification rate measurements performed on HeLa cells treated with either cl-SCRpep or cl-HK2pep (200 nM; mean ± SEM, *n* = 3 independent experiments, Student's *t*-test analysis n.s.).

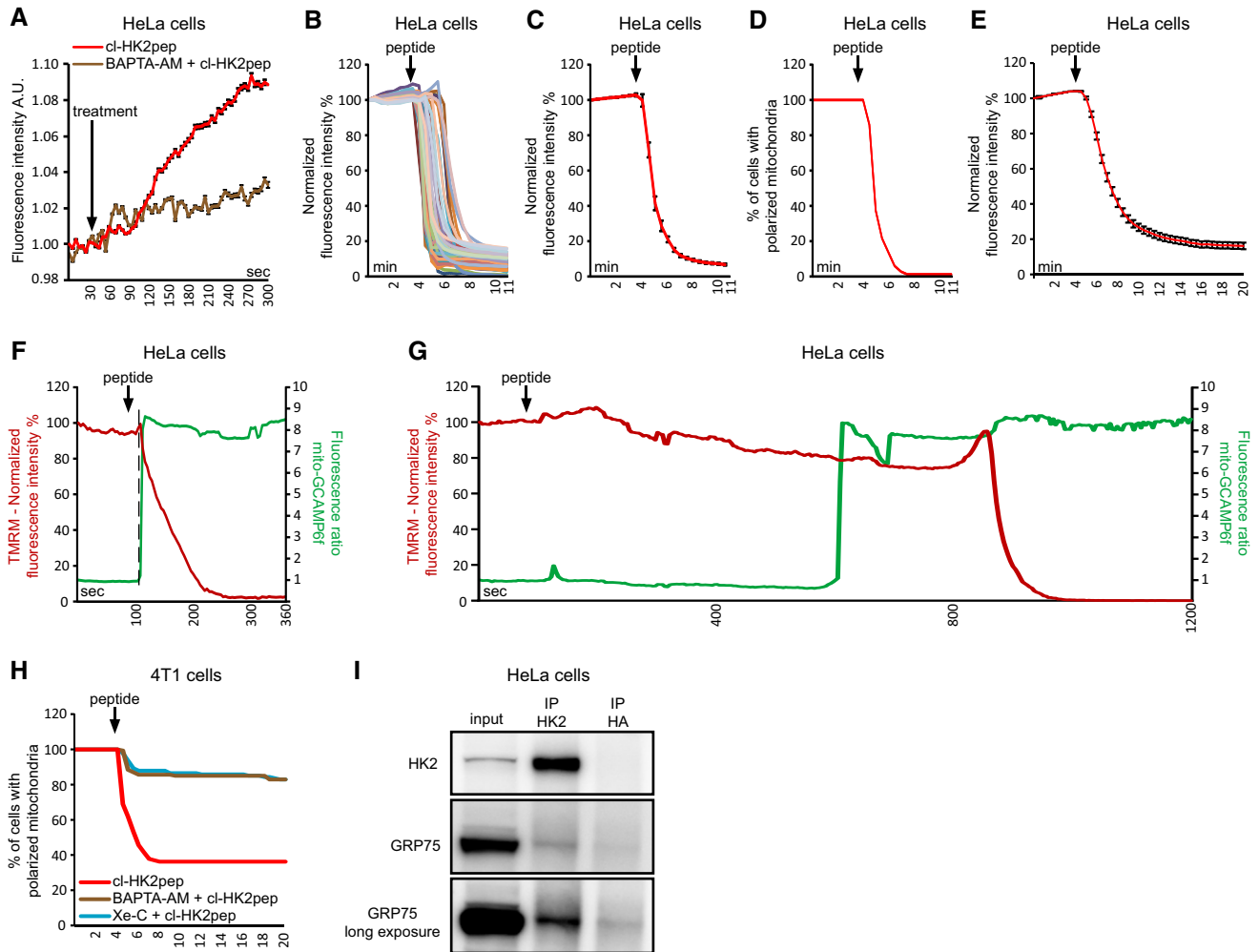


**Figure EV3. Related to Fig 2. Kinetics of cl-HK2pep-induced mitochondrial depolarization.**

- A** IP<sub>3</sub> levels are assessed with the GFP-PHD probe in presence or not of 10  $\mu$ M BAPTA-AM; data are reported as mean of fluorescent signals  $\pm$  SEM ( $n = 3$  independent experiments)
- B–E** Changes in mitochondrial membrane potential following cl-HK2pep treatment assessed with TMRM as in Fig 2G. In B and C, HeLa cells are treated with 5  $\mu$ M cl-HK2pep; mitochondrial depolarization is shown for single cells (B;  $n = 60$  cells analyzed from three independent experimental days) or as an averaged trace (C;  $n = 60$  cells analyzed from three independent experimental days). TMRM signal is normalized to the initial value and expressed in percentage for each time point. D, TMRM positive HeLa cells are expressed in percentage (threshold count: fluorescence signal > 40% of initial value;  $n = 60$  cells analyzed from three independent experimental days). E, HeLa cells are treated with 2  $\mu$ M cl-HK2pep ( $n = 216$  cells analyzed from 10 independent experimental days; fluorescence mean  $\pm$  SEM) and analyzed as in C.
- F, G** Changes in Ca<sup>2+</sup> levels and membrane potential in HeLa cell mitochondria following treatment with 2  $\mu$ M cl-HK2pep. Measurements are performed in parallel on cells expressing mito-GCAMP6f and loaded with TMRM. Two different single representative cell traces are shown, characterized by fast (F) or slow (G) mitochondrial depolarization following peptide treatment (three different experimental days). The dotted line indicates the time point in which mito-GCAMP6f ratio increases from the basal.
- H** Mitochondrial depolarization in 4T1 cells treated with 2  $\mu$ M cl-HK2pep ( $n = 129$ ) is analyzed as in C. Where indicated, BAPTA-AM (10  $\mu$ M;  $n = 147$ ) or Xe-C (5  $\mu$ M;  $n = 141$ ) are added as in Fig 2B 1 h before experiment.
- I** Co-immunoprecipitation between HK2 and GRP75.

**Figure EV4. Related to Fig 3. Cell death induction by cl-HK2pep in different cancer cell models and in non-tumorigenic cell models.**

- A, B Effect of a 1 h glucose deprivation and of HK2 inhibition by 5-thio-glucose or 2-deoxy-glucose (10 mM each, 1 h pre-incubation) on death induced in HeLa cells by a 15-min treatment with 5  $\mu$ M cl-HK2pep. Cell death is assessed as in Fig 3C (mean  $\pm$  SD  $n = 3$  independent experiments).
- C–E Effect of the pan-caspase inhibitor Z-VAD-fmk (50  $\mu$ M) on death elicited in HeLa, CT26, and 4T1 cells by a 15-min treatment with 5  $\mu$ M cl-HK2pep. Cell death is assessed as in Fig 3C (mean  $\pm$  SD  $n = 3$  independent experiments).
- F, G The effect of the pan-calpain inhibitor PD150606 (50  $\mu$ M) on mitochondrial depolarization elicited by 5  $\mu$ M cl-HK2pep is measured as in Fig 3B ( $n = 3$  independent experiments in each cell line; mean percentage of dead cells is normalized to time 0  $\pm$  SD; two-way ANOVA:  $P < 0.0001$ , cl-HK2pep treatment versus cl-HK2pep+PD150606 or cl-SCRpep treatments; Bonferroni post-test in graphs  $***P < 0.001$ ).
- H–L The effect of PD150606 on cell death elicited by treatment with 5  $\mu$ M cl-HK2pep in CT26, 4T1, COLO 741, MDA-MB-231, and MEC1 cancer cell models is analyzed as in Fig 3F. Data  $\pm$  SD are analyzed with a two-way ANOVA:  $P < 0.0001$ , cl-HK2pep treatment versus cl-HK2pep+PD150606 or cl-SCRpep treatments; Bonferroni post-test in graphs  $***P < 0.001$ . In experiments throughout the figure, cl-SCRpep is used as a negative control;  $n \geq 3$  independent experiments for each cell line.
- M Western immunoblot analysis of HK2 levels in murine cell models (colon carcinoma CT26 cells, breast cancer 4T1 cells, macrophage RAW 264.7 cells, and myoblast C2C12 cells). ATP5A and GAPDH are mitochondrial and cytosolic loading controls, respectively.
- N Fluorescence co-staining of HK2 and split-GFP-based probe for ER-mitochondria contacts (SPLICS<sub>1</sub>) on C2C12 myoblasts and RAW264.7 macrophages. HK2 is revealed with an AlexaFluor555-conjugated secondary antibody. SPLICS<sub>1</sub>-HK2 co-localization is quantified in the bar graph on the right (mean  $\pm$  SD, three independent experiments). Scale bar, 20  $\mu$ m.
- O, P Effect of cl-HK2pep (2 and 5  $\mu$ M) on cell death in RAW 264.7 and C2C12 non-transformed cells. Cell death is assessed by cytofluorimetry as in Fig 3C (mean  $\pm$  SD, three independent experiments).
- Q Effect of cl-HK2pep (10  $\mu$ M) on cell death in rat not tumorigenic hepatocytes. Cell death is assessed by cytofluorimetry as in Fig 3C (mean  $\pm$  SD, three independent experiments).

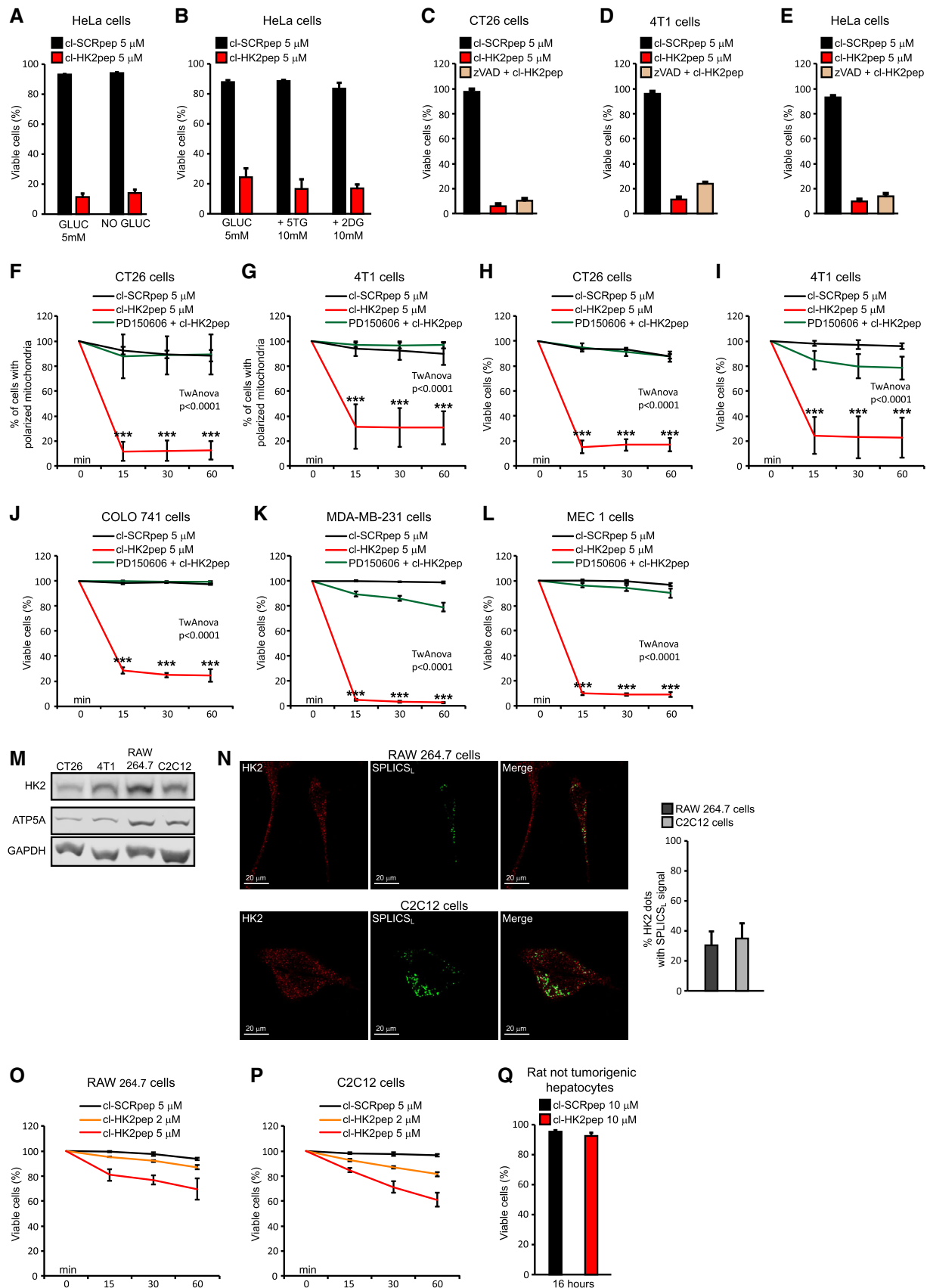


Figure EV4.

**Figure EV5. Related to Fig 5. Analysis of mouse samples following xenograft injection of tumor cells and peptide treatment.**

- A Western immunoblot analysis of MMP2 and MMP9 expression in neoplasms formed by 4T1 cells in mouse allografts; TOM20 is used as loading control.
- B Body weight measurements of mice from experiments reported in Fig 5F–H (from left to right, respectively—mean  $\pm$  SD; F: CNT  $n = 4$ ; cl-HK2pep  $n = 5$ ; HK2pep  $n = 5$  mice; G: SCRpep  $n = 6$ ; HK2pep  $n = 7$  mice; H: SCRpep  $n = 5$ ; HK2pep  $n = 7$  mice).
- C, D Effect of HK2-targeting on *in vivo* neoplastic growth. Intraperitoneal administration of HK2pep (C; 5 injections of 60 nmol peptide every 12 h; SCRpep  $n = 6$ ; HK2pep  $n = 7$ ) reduce neoplastic growth; the same effect is observed on allografts of breast carcinoma 4T1 cells (D; 5 injections of 60 nmol peptide every 12 h; SCRpep  $n = 5$ ; HK2pep  $n = 7$ ) in Balb/c female mice. A two-way ANOVA is performed ( $P < 0.0001$ -HK2pep versus SCRpep during the time); Bonferroni post-test in the graphs \* $P < 0.05$ ; \*\*\* $P < 0.001$ .
- E Representative hematoxylin/eosin staining on samples from heart, skeletal muscle, kidney, and spleen obtained from mice-bearing CT26 tumors after peptide treatment as in Fig 5G. Scale bar: 200  $\mu\text{m}$ .
- F Cell death and mitosis analyses on tumor slices from Fig 5G experiment. Dead or mitotic cells were counted on samples stained with hematoxylin/eosin (SCRpep versus HK2pep; mitotic cells count:  $P < 0.001$  with Student's *t*-test; dead cell count:  $P < 0.05$  with Student's *t*-test; at least 10 different fields where counted for each tumor samples). Scale bar: 100  $\mu\text{m}$ .

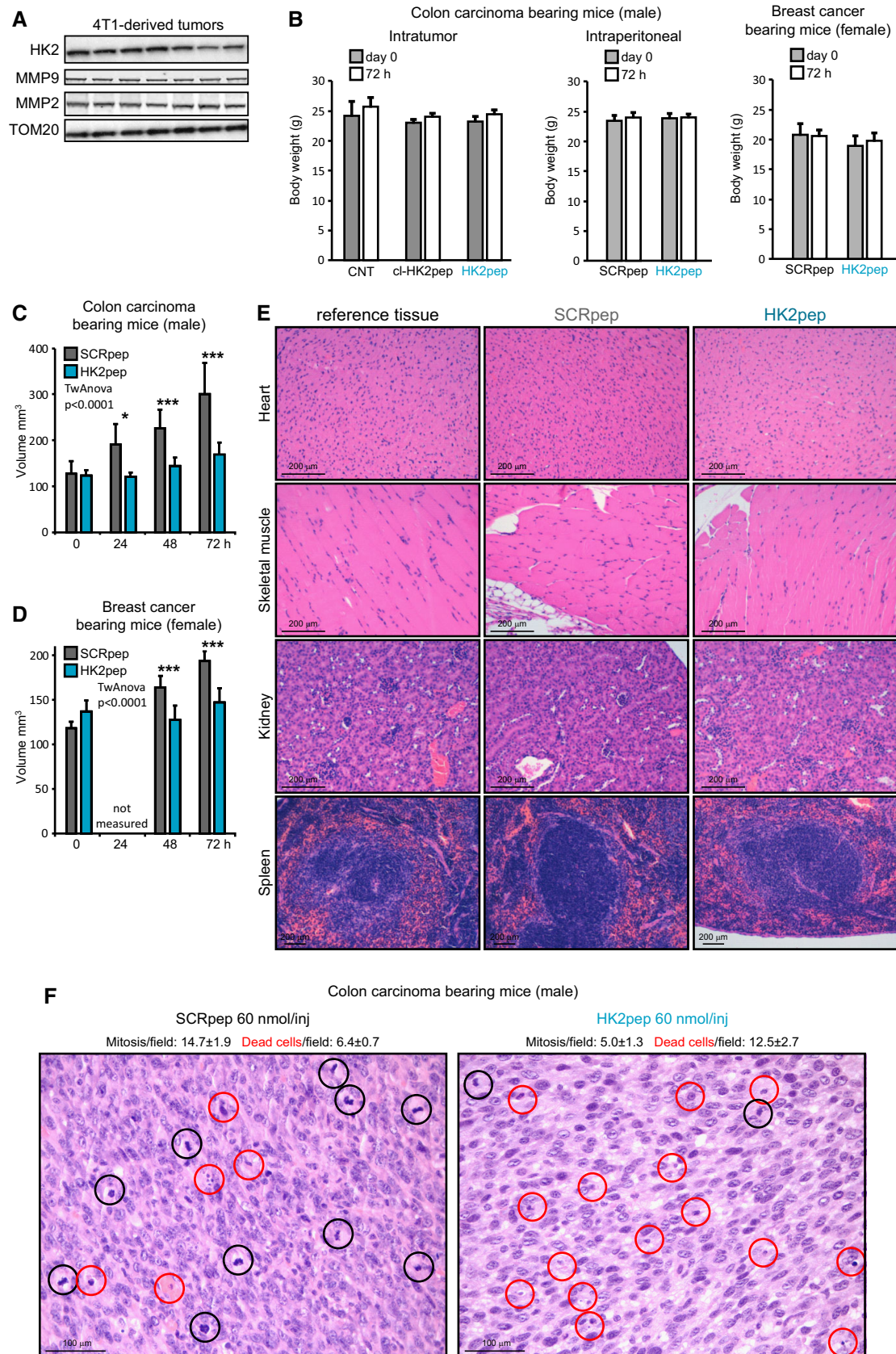


Figure EV5.